

## Synchronization of a conservative map

Liu Zonghua<sup>1,2,3</sup> and Chen Shigang<sup>4</sup>

<sup>1</sup>CCAST (World Laboratory), P.O. Box 8730, Beijing 100080, People's Republic of China

<sup>2</sup>Graduate School, China Academy of Engineering Physics, P.O. Box 8009, Beijing 100088, People's Republic of China

<sup>3</sup>Department of Physics, Guangxi University, Nanning 530004, People's Republic of China

<sup>4</sup>Institute of Applied Physics and Computational Mathematics, P.O. Box 8009, Beijing 100088, People's Republic of China

(Received 14 January 1997)

We demonstrate that two identical chaotic systems of a conservative map can be synchronized by applying periodic pulses at regular time intervals. This idea is illustrated with a two-dimensional standard map. The mechanism is also studied. [S1063-651X(97)08608-X]

PACS number(s): 05.45.+b, 03.20.+i, 46.10.+z

Synchronization is a widespread phenomenon occurring in different fields. Numerous applications of the synchronization in mechanics, electronics, communication, measurements, and in many other fields have shown that synchronization is extremely important in engineering. On the other hand, the phenomenon of synchronization in biology is very interesting. One of the most cited examples is given by the southeastern fireflies, where a large number of insects gathered on trees flash all together [1]. Other examples include crickets exchanging chirps, cardiac cells interacting with voltage pulses, neurons receiving and sending synaptic pulses, etc.

The progress in studies of nonlinear dynamical systems significantly extended the concept of synchronization. It was shown that synchronization can be associated not only with regular behavior, such as periodic or quasiperiodic oscillations, but also with chaotic behavior. Numerous papers, published in the past six years, employed the ideas of synchronized chaos for different techniques of communications with chaos, chaos suppression, and monitoring dynamical systems. The pioneering work is that of Pecora and Carroll [2]. Shortly afterwards many related methods were presented, such as the parameter perturbations approach [3], the modified Pecora and Carroll method [4,5], the feedback method [6,7], etc. The Pecora and Carroll idea of synchronization has been extended to coupled systems [8], even to the case of generalized synchronization [9,10] where the driving and response system are different. Rulkov *et al.* [10] generalize the idea of synchronization equating variables from the response with a function of the variables of the drive. However, all these methods are designed for the dissipative systems. As we know, only two references [11,12] discussed the case of a conservative map. Here we will discuss the synchronization of the Hamiltonian chaos and use the standard map, perhaps the most widely known example of a chaotic Hamiltonian system, as an example to demonstrate the process of synchronization.

Recently, Refs. [13,14] present a method which uses a wait-and-reset strategy for synchronizing chaotic systems. In this paper, we extend this method to a Hamiltonian system and call it the periodic impulsive method. Consider the standard map

$$r_{n+1} = r_n - \frac{\kappa}{2\pi} \sin 2\pi x_n, \quad \text{mod } 1$$

$$x_{n+1} = x_n + r_{n+1}, \quad \text{mod } 1. \quad (1)$$

Obviously, its Jacobian determinant equals one, so it is a conservative map. The standard map has a straightforward physical interpretation. It is the Poincaré return map for a frictionless periodically kicked pendulum. With the increasing of parameter  $\kappa$ , the system undergoes the transition from local to global chaos. The critical value of parameter  $\kappa$  is 0.971 635 4. At this value of  $\kappa$ , the last remaining KAM torus which stretches horizontally from  $x=0$  to  $x=1.0$  is broken. For the values of  $\kappa > 0.971 635 4$ , the system demonstrates global chaos. In this paper, we let  $\kappa = 1.171 635 4$ . Consider an identical system with Eq. (1)

$$r'_{n+1} = r'_n - \frac{\kappa}{2\pi} \sin 2\pi x'_n, \quad \text{mod } 1$$

$$x'_{n+1} = x'_n + r'_{n+1}, \quad \text{mod } 1. \quad (2)$$

Following Pecora and Carroll's method, we call Eq. (1) the driving system and Eq. (2) the response system. Reference [11] indicated that it is possible to synchronize the standard map by using variable  $r$  as a drive variable and not possible by using variable  $x$  as a drive variable. This naturally raises the question: does this then imply that it is impossible to synchronize two systems using  $x$  as the drive signal? In fact, we will demonstrate that, perhaps quite contrary to one's intuition, synchronization using  $x$  as a key is possible if, instead of continuously monitoring the response system, one is willing to wait for a short while before each attempt to reset the response system. Now we use the periodic impulsive method to implement the synchronization. In this paper we discuss the synchronization of three cases, they are the synchronization of chaotic, quasiperiodic, and periodic orbits. Firstly, we consider the case of chaotic orbits and add periodic pulse to variable  $x'$ . The second equation of Eq. (2) becomes

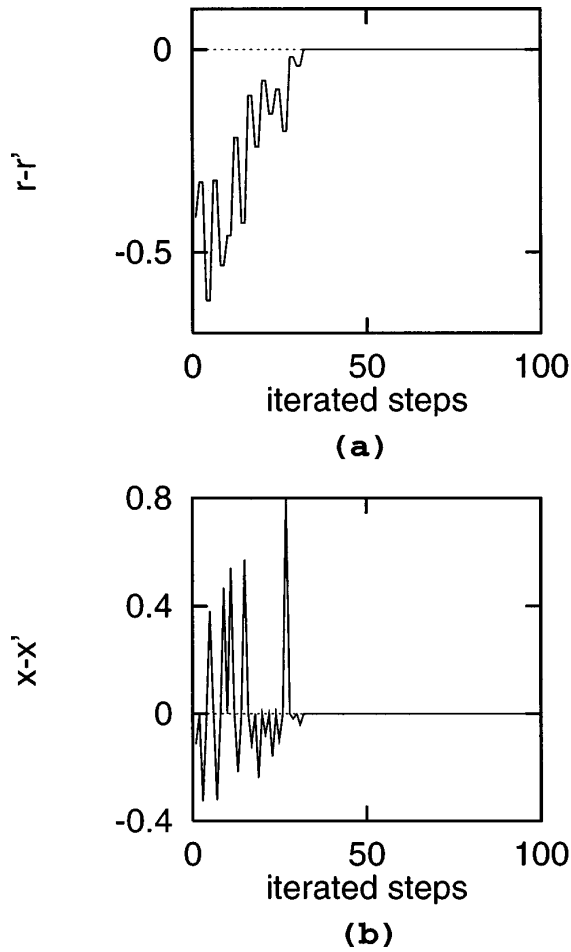


FIG. 1. Synchronization of chaotic orbits. The periodic pulse is added to variable  $x'$ . The initial point of the driving system is 0.1, 0.6, and the initial point of the response system is 0.8, 0.3. (a) Evolution of variable  $r$  when  $\Delta n=2$ . (b) Evolution of variable  $x$  when  $\Delta n=2$ .

$$\begin{aligned} x'_{n+1} &= x'_n + r'_{n+1}, & n \neq j\Delta n \\ x'_{n+1} &= x_{n+1}, & n = j\Delta n \end{aligned} \quad (3)$$

where  $j$  runs over natural numbers, implying that the kicks are applied at intervals that are uniformly spaced by  $\Delta n$ . During  $\Delta n-1$  iteration steps the response system evolves over the original map (2), while at the next step the state variable  $x'_i$  is replaced by the value of the state variable  $x_i$  of the driving system, that is,  $x'_i = x_i$ . In other words, the dynamical system (2) oscillates freely and independently from the driving system (1) except for the moments when the variable  $x'_i$  is forced to the new value  $x_i$ . In our numerical simulation, we observe that the synchronization can be implemented only when  $\Delta n=2$  or 3. Figure 1 shows the result when the initial point of the driving system is (0.1, 0.6) and the initial point of the response system is (0.8, 0.3). From Fig. 1 one can see that the implementation of synchronization only needs about 30 steps when  $\Delta n=2$ . It illustrates that the periodic impulsive method can do what the Pecaro and Carroll's method [11] cannot do.

For the case of adding periodic pulse to variable  $r'$ , the first equation of Eq. (2) becomes

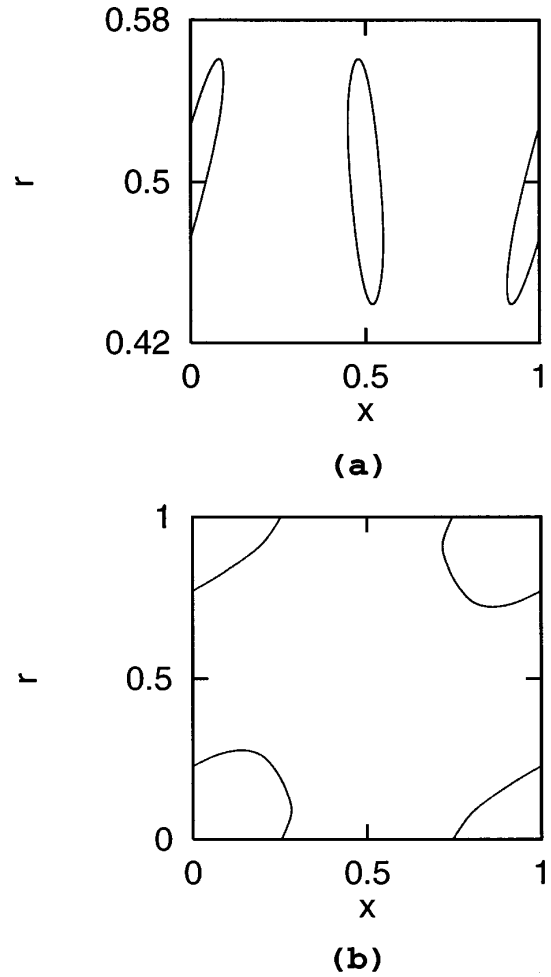


FIG. 2. Two quasiperiodic orbits. (a) The initial point is  $r_0=0.515\ 035\ 398\ 828\ 775\ 0$ ,  $x_0=0.451\ 249\ 476\ 513\ 977\ 4$ , (b) the initial point is  $r_0=0.275\ 312\ 253\ 843\ 563\ 1$ ,  $x_0=0.111\ 993\ 390\ 277\ 928\ 2$ .

$$r'_{n+1} = r'_n - \frac{\kappa}{2\pi} \sin 2\pi x'_n, \quad n \neq j\Delta n$$

$$r'_{n+1} = r_{n+1}, \quad n = j\Delta n \quad (4)$$

where the meanings of  $j, \Delta n$ , and the values of the initial points are just the same as that of Eq. (3). The response system (2) and the driving system (1) satisfy the same equation except that the variable  $x'_i$  is reset to  $x_i$  at a regular iterated interval  $\Delta n$ . (The traditional synchronization scheme corresponds to taking  $\Delta n=1$ .) Our numerical simulation shows that the two systems can be synchronized only when  $\Delta n=2, 3$ , or 4 except for  $\Delta n=1$ . (That is the case of Ref. [11].) On the other hand, if the drive system chooses different initial points, the synchronized steps are different. It means that the synchronized steps have something to do with the initial point of the drive system. We will explain these phenomena later.

It must be pointed out that the response system (2) has become a dissipative system when using periodic pulses (3) or (4). Considering  $\Delta n$  steps as a unit, its Jacobian in  $\Delta n$  steps is  $J = \prod_{i=1}^{\Delta n} J_i$ , where

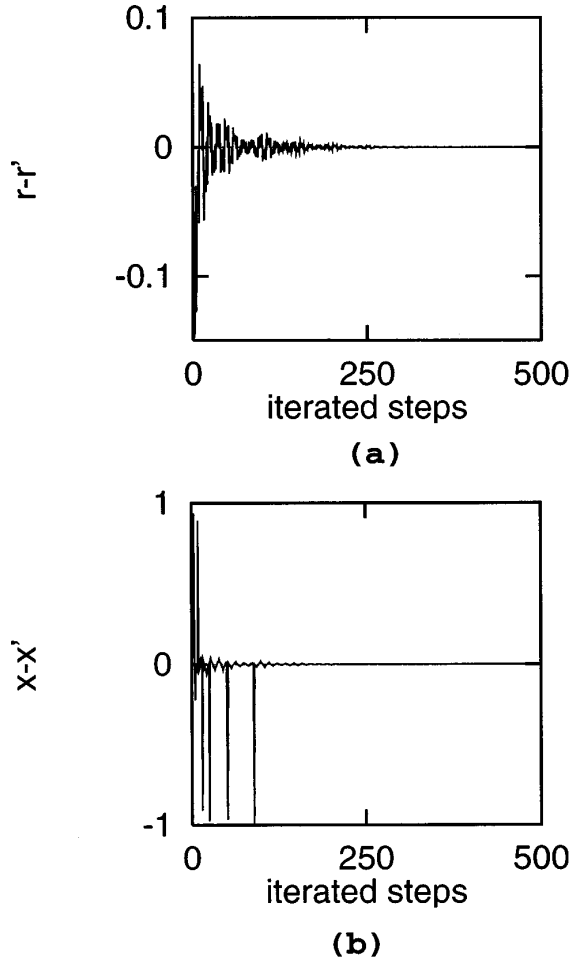


FIG. 3. The synchronization of quasiperiodic orbit corresponding to Fig. 2(a). The periodic pulse is added to variable  $x'$ . The initial point of the response system is  $(0.7, 0.2)$  and  $\Delta n = 6$ .

$$J_i = \begin{pmatrix} 1 & -\kappa \cos 2\pi x'_i \\ 1 & 1 - \kappa \cos 2\pi x'_i \end{pmatrix}, \quad i = 1, \dots, \Delta n - 1$$

$$J_{\Delta n} = \begin{pmatrix} 1 & -\kappa \cos 2\pi x'_{\Delta n} \\ 0 & 0 \end{pmatrix}, \quad \text{for Eq. (3)} \quad (5)$$

$$J_{\Delta n} = \begin{pmatrix} 0 & 0 \\ 1 & 0 \end{pmatrix}, \quad \text{for Eq. (4)}.$$

Obviously, the Jacobian determinant  $|J| = 0$ , so that the response system has become a dissipative system. Otherwise, synchronization cannot be implemented for the conservative map.

Secondly, we consider the case of quasiperiodic orbits. By careful research we find two quasiperiodic orbits in Fig. 2. The initial point of Fig. 2(a) is  $r_0 = 0.515\,035\,398\,828\,775\,0$ ,  $x_0 = 0.451\,249\,476\,513\,977\,4$  and the initial point of Fig. 2(b) is  $r_0 = 0.275\,312\,253\,843\,563\,1$ ,  $x_0 = 0.111\,993\,390\,277\,928\,2$ . We let the driving system (1) run along the quasiperiodic orbit, and give the response system (2) an initial point  $(r'_0 = 0.7, x'_0 = 0.2)$ . We have observed that synchronization can be implemented by both Eqs. (3) and (4). For the quasiperiodic orbit of Fig. 2(a), we observe that in Eq. (3) syn-

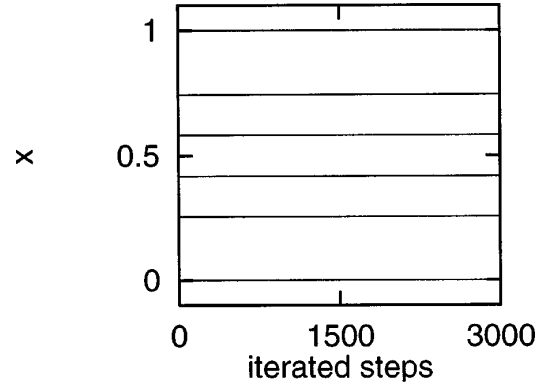


FIG. 4. A period-five orbit. One point of period five is  $r_0 = 0.512\,277\,623\,087\,423\,1$ ,  $x_0 = 0.256\,155\,537\,624\,807\,5$ .

chronization can be implemented only when  $\Delta n = 2, 5-8, 11-14, 17-20, 23-24$ , etc., and in Eq. (4) only when  $\Delta n = 1, 3-4, 7-10, 13-14, 16-17, 19-20, 22, 25-26$ , etc. For the quasiperiodic orbit of Fig. 2(b), we observe that in Eq. (3) synchronization can be implemented only when  $\Delta n = 2-4, 6$ , and in Eq. (4) only when  $\Delta n = 1-3, 5, 7$ . Figure 3 shows the result of corresponding to Fig. 2(a) when periodic pulses are added to variable  $x'$  and  $\Delta n = 6$ . From Fig. 3 one can see that the synchronized steps are about 300.

Lastly, we consider the case of periodic orbits. Because the conservative maps have no attractive basin, this leads to some difficulty in finding the periodic orbits. But fortunately there are four symmetry lines for the standard map,  $x = 0, \frac{1}{2}, r/2, (r+1)/2$ . At least two of the  $M$  points on a period- $M$  cycle will fall on the symmetry lines. Along the symmetry lines one can quickly find one point of the period- $M$  orbit using a Newton-Raphson algorithm. Figure 4 shows the result of a period 5, where one point of period 5 is  $r_0 = 0.512\,277\,623\,087\,423\,1$ ,  $x_0 = 0.256\,155\,537\,624\,807\,5$ . It must be pointed out that in Fig. 4 the line of  $x = 0$  and the line  $x = 1$  are just the same because of the mod 1 in Eq. (1). Now we let the driving system run along the period-five orbit, and give the response system (2) an initial point  $(r'_0 = 0.7, x'_0 = 0.2)$ . We observe that in Eq. (3) synchronization can be implemented only when  $\Delta n = 2, 4$ , and in Eq. (4) only when  $\Delta n = 1, 3, 5, 7, 11-13$ .

To understand why such a synchronization scheme might work, we now study the conditional Lyapunov exponents of the response system. Rewrite Eq. (2) as

$$r_{n+1} = f_1(r_n, x_n),$$

$$x_{n+1} = f_2(r_n, x_n). \quad (6)$$

If the periodic pulse is applied to Eq. (6) after  $\Delta n$  times, one can consider the  $\Delta n$  steps as a unit. Then a new map is created

$$r_{m+1} = F_1(r_m, x_m),$$

$$x_{m+1} = F_2(r_m, x_m), \quad (7)$$

where  $F_1 = f_1^{\Delta n}$ ,  $F_2 = f_2^{\Delta n}$ . The periodic pulse added in Eq. (6) is equivalent to Eq. (7) having a drive variable. If the periodic pulse is applied to variable  $r$ , we have

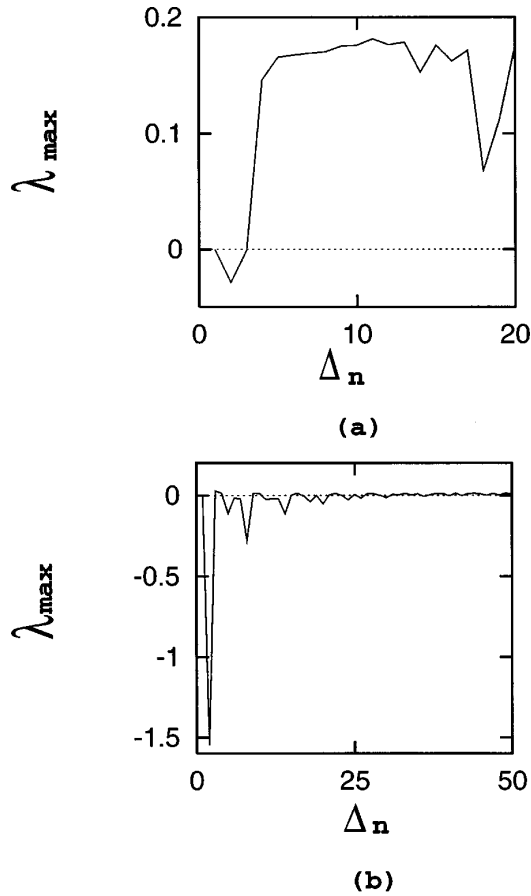


FIG. 5. Maximum Lyapunov exponent spectra of the response system corresponding to Eq. (3). (a) The driving system is chaotic with initial point 0.1,0.6, (b) the driving system is Fig. 2(a).

$$\delta x_{m+1} = \frac{\partial F_2}{\partial x_m} \delta x_m$$

$$\lambda_x = \lim_{m \rightarrow \infty} \frac{1}{m} \sum_{j=0}^{m-1} \ln \left| \frac{\partial F_2}{\partial x_j} \right| = \lim_{m \rightarrow \infty} \frac{1}{m} \sum_{j=0}^{m-1} \ln \left| \frac{\partial f_2^{\Delta n}}{\partial x_j} \right|, \quad (8)$$

Similarly, if the periodic pulse is applied to variable  $x$ , we have

$$\lambda_r = \lim_{m \rightarrow \infty} \frac{1}{m} \sum_{j=0}^{m-1} \ln \left| \frac{\partial f_1^{\Delta n}}{\partial r_j} \right|, \quad (9)$$

where  $\lambda_x$  and  $\lambda_r$  represent the conditional Lyapunov exponents corresponding to the case of adding pulses. Obviously,  $\lambda_x$  and  $\lambda_r$  depend on  $\Delta n$ . When  $\lambda_x$  or  $\lambda_r < 0$ , synchronization can be implemented; otherwise, synchronization cannot be implemented. This is the reason that there are gaps in successive values of  $\Delta n$ .

On the other hand,  $\lambda_x$  and  $\lambda_r$  are related to the property of trajectory, i.e., the chaotic, quasiperiodic, or periodic orbit. Taking  $\Delta n = 2$  as an example, we have

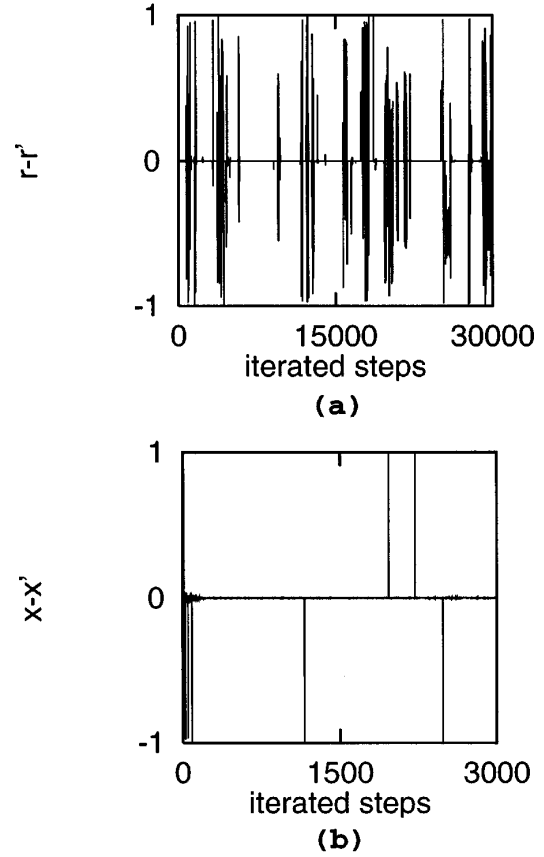


FIG. 6. The effect of noise is shown. (a) Corresponding to Fig. 1(a). The intensity of the noise is  $1.0 \times 10^{-8}$ . (b) Corresponding to Fig. 3(a). The intensity of the noise is  $1.0 \times 10^{-4}$ .

$$\lambda_x = \lim_{m \rightarrow \infty} \frac{1}{m} \sum_{j=0}^{m-1} \ln \left| 1 - 2\kappa \cos(2\pi x_j) - \kappa [1 - \kappa \cos(2\pi x_j)] \cos 2\pi \left( x_j + r_j - \frac{\kappa}{2\pi} \sin(2\pi x_j) \right) \right|,$$

$$\lambda_r = \lim_{m \rightarrow \infty} \frac{1}{m} \sum_{j=0}^{m-1} \ln \left| 1 - \kappa \cos 2\pi \left( x_j + r_j - \frac{\kappa}{2\pi} \sin(2\pi x_j) \right) \right|. \quad (10)$$

For the chaotic trajectory,  $x_j$  and  $r_j$  have ergodicity. The sums of Eq. (10) can be substituted by integration on the phase space, as in Ref. [11]. However, for the quasiperiodic or periodic orbits, the summing of Eq. (10) can only be calculated along a special orbit. So the synchronized steps has something to do with the initial point of the drive system. For studying the relation between synchronization and  $\Delta n$  we have calculated the maximum Lyapunov exponent of the response system. We find that the maximum Lyapunov exponents are negative for those  $\Delta n$  in which synchronization can be implemented and positive for those  $\Delta n$  in which synchronization cannot be implemented. This is consistent with Pecora and Carroll's theorem [2]. Figure 5 shows the results corresponding to Eq. (3).

To test the effect of external noise on synchronization in the model studied here, we have studied how synchronization is affected by a white noise. We consider the Gaussian

white noise  $\xi$  having zero mean and standard deviation equal to one, generated by using the Box-Müller method [15], and introduce noise in the form

$$r_i = r_i(1.0 + \rho\xi), \quad (11)$$

or

$$r_i = r_i + \rho\xi, \quad (12)$$

where  $\rho$  denotes the intensity of external noise. This noise is applied at each iterated step. Figure 6(a) shows the result corresponding to Fig. 1(a) when using Eq. (11) and Fig. 6(b) shows the result corresponding to Fig. 3(a) when using Eq. (12). To others  $\Delta n$  or adding noise to variable  $x'$ , our numerical simulation shows that the results are just the same as Fig. 6. From Fig. 6 one can see that synchronization is occasionally disrupted by the short time large order burst. This corresponds to the case of on-off intermittency in that the deviation lies at nearly zero value for a long period of time, which is interrupted by the short time burst of nonzero value. The reason for the burst has something to do with mod1 in Eqs. (1) and (2). By checking the data file we find that the intermittency always first emerges at the neighborhood of variables  $r$  or  $x$  equaling zero or one, and then lasts a short time. When variable  $r$  or  $x$  is near zero or one, the effect of the external noise becomes extremely important. A small noise might let the variables of the driving system or response system change about 1 because of mod1 in Eqs. (1) and (2). It seriously destroys synchronization between the driving and response system and induces the burst.

On the other hand, with the increasing of the intensity of external noise the intermittency emerges more frequently.

Our numerical experiments discover that there is some power law between the intensity of external noise and the percentage of synchronization, where part of the intermittency is removed. The exponent of the power law is a small constant number when the intensity of the external noise is small and a greater constant number when the intensity of the external noise is big. This power law exists in all synchronized orbits. For example, for the case of Fig. 6(a) the exponent of the power law is  $-0.06$  when the intensity of the external noise is smaller than  $1.0 \times 10^{-6}$  and  $-0.29$  when the intensity of external noise is greater than  $1.0 \times 10^{-5}$ . For the case of Fig. 6(b) the exponent of the power law is  $-0.2$  when the intensity of the external noise is smaller than  $1.0 \times 10^{-3}$ , and  $-0.946$  when the intensity of the external noise is greater than  $1.0 \times 10^{-3}$ .

In conclusion, we have extended the periodic impulsive method to the conservative map and find that synchronization can be implemented not only in chaotic orbits but also in quasiperiodic or periodic orbits. The method used in Ref. [11] is just a special case of this method. The mechanism that makes this method work is studied. In the process of synchronizing, the driving system is conservative and the response system is dissipative. When synchronization is implemented, both the driving and response systems are conservative. Furthermore, it easily leads to on-off intermittency in the presence of external noise.

#### ACKNOWLEDGMENTS

This work was partially supported by the National Natural Science Foundation of China and the Science Foundation of the China Academy of Engineering Physics.

- 
- [1] S. Bottani, Phys. Rev. E **54**, 2334 (1996).
  - [2] L. M. Pecora and T. L. Carroll, Phys. Rev. Lett. **64**, 821 (1990).
  - [3] Y.-C. Lai and C. Grebogi, Phys. Rev. E **47**, 2357 (1993).
  - [4] L. Kocarev and U. Parlitz, Phys. Rev. Lett. **74**, 5028 (1995).
  - [5] U. Parlitz, L. Kocarev, T. Stojanovski, and H. Preckel, Phys. Rev. E **53**, 4351 (1996).
  - [6] K. Pyragas, Phys. Lett. A **181**, 203 (1993).
  - [7] T. Kapitaniak, Phys. Rev. E **50**, 1642 (1994).
  - [8] N. F. Rulkov *et al.*, Int. J. Bifurcation Chaos Appl. Sci. Eng. **2**, 669 (1992).
  - [9] H. D. I. Abarbanel, N. F. Rulkov, and M. M. Sushchik, Phys. Rev. E **53**, 4528 (1996).
  - [10] N. F. Rulkov *et al.*, Phys. Rev. E **51**, 980 (1995).
  - [11] J. F. Heagy and T. L. Carroll, CHAOS **4**, 385 (1994).
  - [12] C. Tresser, P. A. Worfolk, and H. Bass, CHAOS **5**, 693 (1995).
  - [13] Y.-Y. Chen, Phys. Lett. A **221**, 34 (1996).
  - [14] L. Kocarev and U. Parlitz, Phys. Rev. Lett. **77**, 2206 (1996).
  - [15] W. H. Press, B. P. Flannery, S. A. Teukolsky, and W. T. Vetterling, *Numerical Recipes: The Art of Scientific Computing* (Cambridge University Press, New York, 1986).